



Pyrazolidine-3,5-dione derivatives as potent non-steroidal agonists of farnesoid X receptor: Virtual screening, synthesis, and biological evaluation

Guanghui Deng^{a,†}, Weihua Li^{a,†}, Jianhua Shen^{a,*}, Hualiang Jiang^{a,b}, Kaixian Chen^a, Hong Liu^{a,*}

^a Drug Discovery and Design Centre, State Key Laboratory of Drug Research, Shanghai Institute of Materia Medica, Graduate School of the Chinese Academy of Sciences, Shanghai Institutes for Biological Sciences, Chinese Academy of Sciences, 555 Zuchongzhi Road, Shanghai 201203, China

^b School of Pharmacy, East China University of Science and Technology, Shanghai 200237, China

ARTICLE INFO

Article history:

Received 9 May 2008

Revised 2 July 2008

Accepted 5 September 2008

Available online 10 September 2008

Keywords:

Farnesoid X receptor
Pyrazolidine-3,5-dione
Virtual screening

ABSTRACT

The identification of a novel pyrazolidine-3,5-dione based scaffold hit compound as Farnesoid X receptor (FXR) partial or full agonist has been accomplished by means of virtual screening techniques. A series of pyrazolidine-3,5-dione derivatives (**1a–u** and **7**) was designed, synthesized, and evaluated by a cell-based luciferase transactivation assay for their agonistic activities against FXR. Most of them showed agonistic potencies and 10 of them (**1a**, **1b**, **1d–f**, **1j**, **1n**, **1t**, **5b**, and **7**) exhibited lower EC₅₀ values than the reference drug CDCA. Molecular modeling studies for the representative compounds **1a**, **1d**, **1f**, **1j**, **1n**, **1u**, **5b**, and **7** were also presented. The novel structural scaffold has provided a new direction for finding potent and selective FXR partial and full agonists (referred to as ‘selective bile acid receptor modulators’, SBARMs).

© 2008 Elsevier Ltd. All rights reserved.

Farnesoid X receptor (FXR) is a member of the superfamily of nuclear receptors and is expressed in the liver and intestine as well as other cholesterol-rich tissues such as the adrenal gland.¹ Three research groups independently identified FXR as a nuclear receptor for bile acids in 1999.^{2–4} As a sensor of bile acids, FXR regulates the expression of several target genes involved in the bile acids biosynthesis and transport. In the liver, FXR indirectly represses the expression of CYP7A1, a key enzyme that catalyzes the rate-limiting step in the conversion of cholesterol into the bile acids.⁵ Activated FXR also positively regulates the expression of genes that encoded proteins in the transport of bile acids, including the intestinal bile acid-binding protein (IBABP) and bile salt export pump (BSEP).^{6,7} Furthermore, FXR is involved in processes such as glucose utilization, inflammation, and cancer deriving from the intricate network of interactions concerning bile acids metabolism.⁸ Thus, FXR is emerging as a particular target for the promising potential treatment of hyperlipidemia, cholelithiasis, cholestasis, and diabetes mellitus.^{9,10}

Over the past few years, many efforts have been dedicated to seek highly potent modulators such as full and partial FXR agonists, which are also referred to as ‘selective bile acid receptor modulators’, SBARMs. A partial agonist relative to a full agonist is defined as a ligand that induces a submaximal response even at full receptor occupancy. Bile acids are the endogenous agonists for FXR, such as chenodeoxycholic (CDCA, Fig. 1) and ursodeoxycholic acid

(UDCA) deserved more than 20 years of research activity culminating with the clinical use in the treatment of gallbladder stones and cholestatic liver diseases.⁸ Based on structural modification of CDCA, Pellicciari et al.¹¹ synthesized 6 α -ethyl-chenodeoxycholic acid (6ECDCA, INT-747) as a highly potent FXR full agonist and is launching phase II trial for the potential treatment of liver diseases, and type 2 diabetes. Upon the side chain modification of CDCA, they also presented some 3 α ,7 α -dihydroxy-24-nor-5 β -cholan-23-amine derivatives as partial agonists against FXR.¹² GW4064 was identified as the first non-steroidal FXR agonist endowed with nanomolar potency through high-throughput screening and combinatorial chemistry approach.¹³ High-throughput screening combined with optimization of benzopyran-based combinatorial library result in the discovery of fexaramine, another structurally diverse non-steroidal FXR agonist.¹⁴ However, although a few different types of synthetic molecular agonist of FXR have been discovered, no drug active against FXR has been approved by the FDA so far. Therefore, it is a great challenge to discover and develop novel compounds as FXR modulators not only for the potential treatment of metabolic syndrome, but also for the etiology research of human disease.^{15,16}

Within our efforts in the study of new FXR agonists, we set up a virtual screening¹⁷ protocol based on crystal structures of FXR in complex with agonists. A series of screening methods including docking, consensus scoring, FlexX scoring, and drug-likeness analysis were used to improve the hit rate.^{18,19} By screening of molecular database SPECS (<http://www.specs.net>) and being followed by biological evaluation, **1a** was identified with an EC₅₀ value of 5.15 μ M for activating FXR in a cell-based luciferase transactiva-

* Corresponding authors. Tel.: +86 21 50807042; fax: +86 21 50807088.

E-mail address: hliu@mail.shcnc.ac.cn (H. Liu).

† These authors contributed equally to this work.

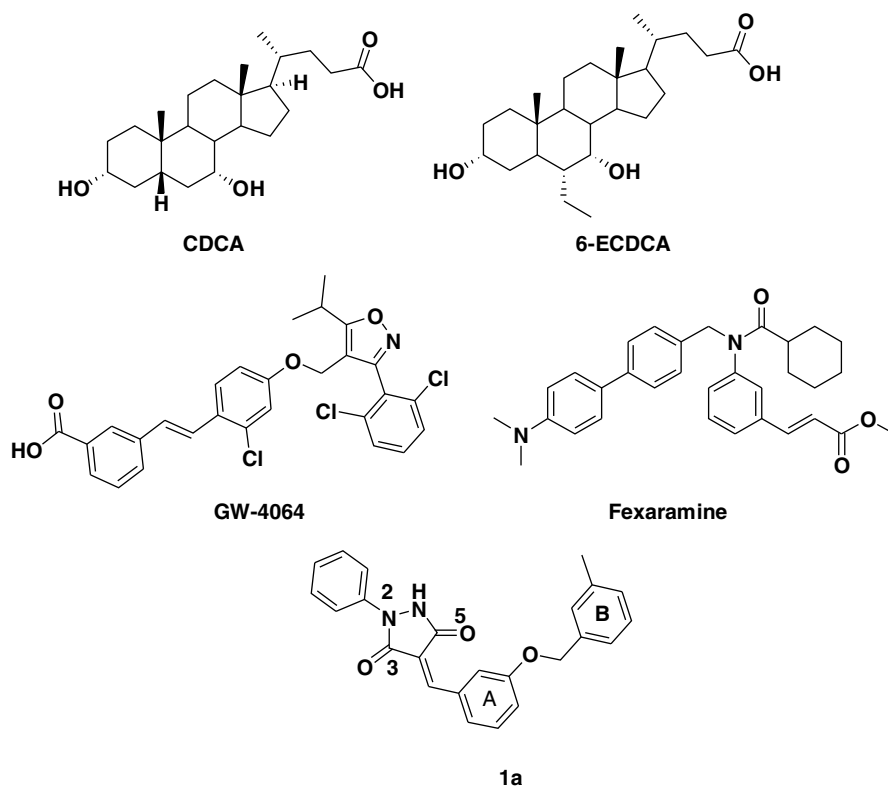


Figure 1. Known FXR agonists and our hit compound **1a**.

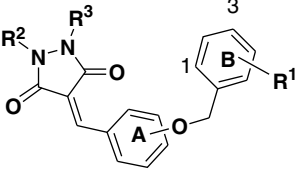
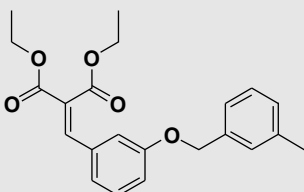
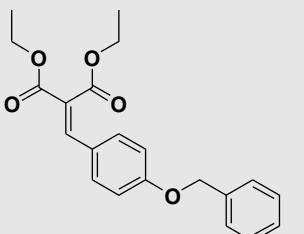
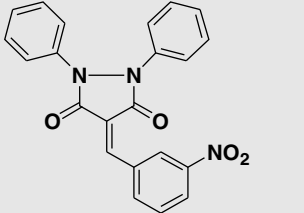
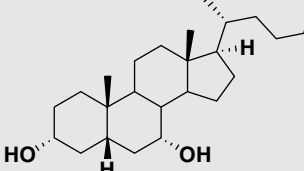
tion assay. Using the hit **1a** as the benchmark compound, a series of novel pyrazolidine-3,5-dione derivatives was designed, synthesized, and evaluated by a cell-based luciferase transactivation assay for their agonistic activities against FXR. Molecular modeling studies were also carried out to investigate their interactions with FXR.

The FXR model used for virtual docking was taken from the coordinate of FXR in complex with fexaramine (PDB entry 1OSH) and the missing coordinates of residues from 271 to 285 were reconstructed based on the corresponding coordinates in the crystal structure of rat FXR-6ECDCA complex (PDB entry 1OSV) using Sybyl version 6.8 (Tripos Inc., 2000). All ligands and ions were removed from the crystal structure of FXR complexes and the FXR model was added with polar hydrogen and Kollman-united-atom charges. A database of over 120,000 compounds (SPECS collection) was assigned with Gasteiger–Marsili charges and was initially screened using the paralleled version of Dock 4.0^{20,21} modified by our laboratory. Residues around the ligand at radius 5 Å in the FXR–fexaramine structure were selected to construct the grids of docking screening. During the execution of Dock 4.0 program, 25 configurations per ligand building a cycle and 50 maximum anchor orientations were used in the anchor-first docking algorithm. All docked configurations were energy minimized using 100 maximum iterations and one minimization cycle. At this stage, the molecules ranked top 5000 in docking energy were selected for further analysis. At the second stage, CScore (Consensus Score) module in Sybyl 6.8 was utilized to re-score the selected molecules. CScore integrates five popular scoring functions for ranking the affinity of ligands bound in the active site of a receptor. Those molecules with CScore above 3 were filtered out. Thus, approximately 2800 molecules were removed after this filter. The remaining 2200 molecules were chosen for further modeling and calculation using FlexX module in Sybyl 6.8. The FlexX program²² considers both the torsion angle flexible and the conformational flexibility of ring

system. In contrast to Dock 4.0, FlexX utilizes an adapted Böhm empirical function to evaluate the ligand–receptor interactions. Those compounds with score ranked top 10% were remained in the hit lists. At this stage, approximately 220 molecules were chosen for further visual inspection and drug-likeness analysis. At the final stage, we restored the selected 220 molecules into the binding pocket of FXR one by one to inspect their locations. The Lipinski's 'rule of 5'.²³ and an additional Chemistry Space Filter²⁴ as filters for drug-likeness analysis were applied on all retrieved compounds and the molecules that violated these rules were eliminated. Following the above steps, 73 molecules were selected and purchased from the SPECS Company and then evaluated by a cell-based luciferase transactivation assay.

Among the 73 molecules, compound **1a**, characterized by a completely new scaffold (Fig. 1), showed a moderate agonistic activity ($EC_{50} = 5.15 \mu M$) and was therefore chosen as the starting point for further structural optimization. Using different substituted benzoyl groups of **1a**, compounds **1b–e** were synthesized (Table 1). Substituting on the N1 and N2 positions of the pyrazolidine-3,5-dione core, compounds **1d–i** were obtained. Changing 3-benzyloxy group with 4-benzyloxy group, compounds **1m–u** were obtained along with phenyl, benzoyl or furoyl substitution on N1 position of pyrazolidine-3,5-dione core. While disubstitution on the N1 and N2 position with phenyl group, replacing the benzyloxy group with NO_2 group and disubstitution on the N1 and N2 positions, compound **7** was achieved. The synthesis of this class of pyrazolidine-3,5-dione derivatives is outlined in Scheme 1. Aldol addition of substituted benzaldehyde **2a** and **2b** with diethyl malonate **3** which were catalyzed by acetic acid and piperazine under refluxing, afforded compounds **4a** and **4b**. Phenolic hydroxyl groups of **4a** and **4b** were alkylated by benzyl chlorides or bromides to produce the desired compounds **5a–e** by the use of microwave in sealed tube. Condensation of **5a–e** with various substituted hydrazine in the presence of NaOEt and EtOH afforded

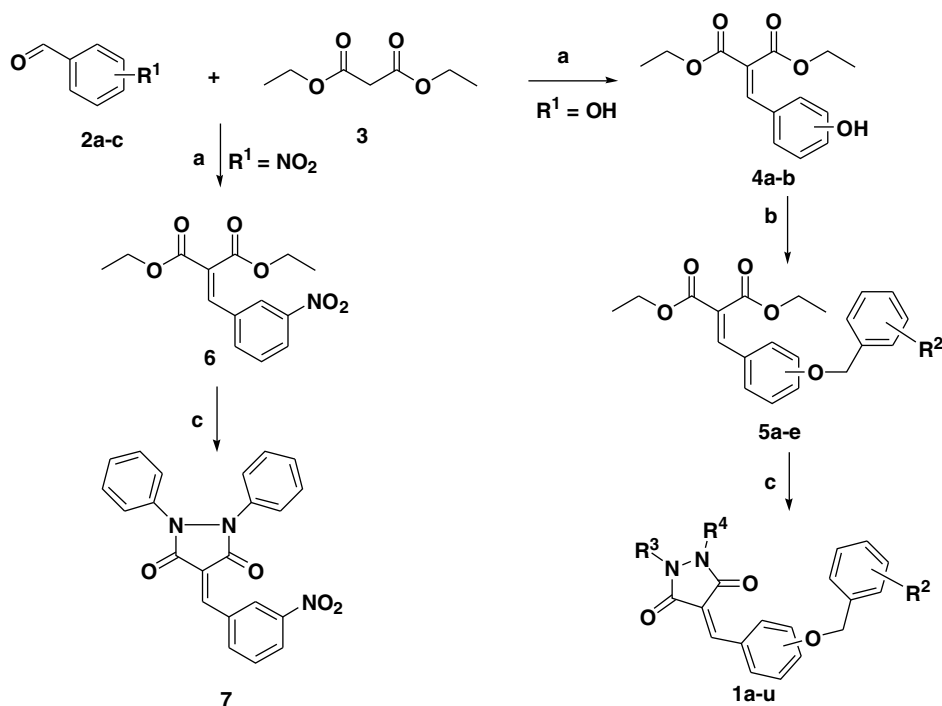
Table 1Structures and agonistic activities against FXR in a cell-based luciferase transactivation assay of pyrazolidine-3,5-dione derivatives in terms of fold activation at 10 μ M

					
Compound	R ¹	R ²	R ³	Substituted position of Ring A	Fold-activity at 10 μ M ^a
1a	3-CH ₃	Phenyl	H	<i>meta</i>	2.88 \pm 0.12
1b	3-F	Phenyl	H	<i>meta</i>	3.17 \pm 0.06
1c	3-CF ₃	Phenyl	H	<i>meta</i>	3.04 \pm 0.06
1d	4-CF ₃	Phenyl	H	<i>meta</i>	3.22 \pm 0.18
1e	3-CH ₃	2-Nitrophenyl	H	<i>meta</i>	3.19 \pm 0.01
1f	3-CH ₃	4-Fluorobenzoyl	H	<i>meta</i>	2.98 \pm 0.24
1g	3-CH ₃	4-Methoxybenzoyl	H	<i>meta</i>	2.32 \pm 0.71
1h	3-CH ₃	Naphthalene-1-carbonyl	H	<i>meta</i>	2.27 \pm 0.42
1i	3-CH ₃	Thiophene-1-carbonyl	H	<i>meta</i>	2.54 \pm 0.36
1j	3-CH ₃	Pyridine-4-carbonyl	H	<i>meta</i>	3.28 \pm 0.22
1k	3-CH ₃	CH ₃	CH ₃	<i>meta</i>	2.61 \pm 0.39
1l	3-CH ₃	H	H	<i>meta</i>	2.41 \pm 0.10
1m	H	Phenyl	H	<i>para</i>	2.34 \pm 0.02
1n	H	Benzoyl	H	<i>para</i>	3.15 \pm 0.13
1o	H	2-Chlorobenzoyl	H	<i>para</i>	2.16 \pm 0.48
1p	H	4-Chlorobenzoyl	H	<i>para</i>	2.48 \pm 0.00
1q	H	4-Bromobenzoyl	H	<i>para</i>	2.25 \pm 0.06
1r	H	4-Methoxybenzoyl	H	<i>para</i>	2.42 \pm 0.15
1s	H	Naphthalene-1-carbonyl	H	<i>para</i>	2.15 \pm 0.46
1t	H	2-Furoyl	H	<i>para</i>	2.93 \pm 0.37
1u	H	Phenyl	Phenyl	<i>para</i>	7.97 \pm 1.35
5a					2.32 \pm 0.29
5b					2.80 \pm 0.08
7					3.15 \pm 0.14
CDCA					10.98 \pm 1.61

^a Values were calculated according to solvents control (as 1-fold). Each data point is the average of triplicate assays. Each experiment was repeated three times.

compounds **1a–u** in 30 min via microwave-assisted reaction. Compound **7** was prepared in the similar procedures without the phenolic hydroxyl-alkylation step.

All derivatives (**1a–u** and **7**, Table 1) and the precursors **5a** and **5b** were evaluated by a cell-based luciferase transactivation assay²⁵ (for details, see Supplementary data) for their agonistic activ-



Scheme 1. Synthetic routes of compounds **1a–u**, **5a**, **5b**, and **7**. Reagents and conditions: (a) HOAc, piperazine, EtOH, reflux, overnight; (b) K_2CO_3 , EtOH, various benzyl chloride, MW, 100 °C, 10 min, sealed tube; (c) NaOEt, EtOH, MW, 140 °C, 30 min, sealed tube.

ities against FXR, using CDCA as the reference drug. As shown in Table 1, all the compounds showed agonistic activities against FXR at 10 μ M, with the fold activation range from 2.15-fold (**1s**) to 7.97-fold (**1u**). Many of them (10 out of 24) had agonistic activities higher than that of the initial lead **1a** (2.88-fold at 10 μ M, EC_{50} = 5.15 μ M). Introducing electron-withdrawing group 3-F, 3- CF_3 , or 4- CF_3 to the benzyloxy group (**1b–d**) resulted in improved activity to 3.17-, 3.04-, and 3.22-fold at 10 μ M, respectively. When the N1 substituent was changed from phenyl group into 2-nitrophenyl group, the activity was improved from 2.88- to 3.19-fold at 10 μ M (**1e**). While, replacing N1 substituent with various acyl groups led to fold-activity ranging from 2.27- to 3.28-fold (**1f–j**). The N1,N2-dimethyl-substituted derivative (**1k**, 2.61-fold at 10 μ M) or N1,N2-unsubstituted derivative (**1l**, 2.41-fold at 10 μ M) showed reduced agonistic activity. Little change in activity was observed by *meta*- or *para*-substitution on the benzyl ring A (**1m–t**). N1,N2-Diphenyl-substituted pyrazolidine-3,5-dione core (**1u**) showed the most potent fold activation (7.97-fold at 10 μ M) among all the synthesized compounds. Surprisingly, the precursor compounds with diethyl malonate moiety instead of pyrazolidine-3,5-dione core along with 4-benzyloxy moiety (**5b**, 2.80-fold at 10 μ M) exhibited positive agonistic activity while the same class along with 3-(3'-methyl)-benzyloxy moiety (**5a**) showed less potent activity (2.32-fold at 10 μ M). Another interesting finding was that the short skeleton compound with 3- NO_2 instead of moiety 3-benzyloxy moiety (**7**, 3.15-fold at 10 μ M) exhibited positive agonistic activity and was even stronger than that of **1a**.

To determine the exact potency of the compounds that demonstrated significant agonistic activities against FXR, 11 compounds were selected for further investigation in concentration–response studies, and the results are summarized in Table 2. All these compounds concentration-dependently activated FXR and showed prominent agonistic activities with concentration at half-maximal stimulation (EC_{50}) values ranging from 1.86 to 6.92 μ M. Among them, seven compounds deserved higher potency than that of the initial hit **1a** and 10 compounds showed higher EC_{50} values

Table 2
Determination of EC_{50} values of selected compounds

Compound	EC_{50} (μ M)
1a	5.15
1b	4.79
1c	6.92
1d	2.04
1e	5.37
1f	1.86
1j	2.40
1n	3.98
1t	3.31
1u	6.31
5b	6.17
7	4.27
CDCA	6.31

than that of CDCA (Table 2). Compound **1f** (EC_{50} = 1.86 μ M) deserved the most potent agonistic activity. As illustrated in Figure 2, compounds **1f**, **1d**, **1j**, and **1u** induced higher activation than that of CDCA at low concentration (below 5 μ M). However, **1d**, **1f**, and **1j** induced a submaximal response compared with CDCA (approximately 3- vs 10.98-fold at 10 μ M). This finding suggested that **1d**, **1f**, and **1j** may act as partial agonists of FXR in this experimental setting. In addition, **1u** exhibits a similar maximal response compared with CDCA (7.97 ± 1.35 - vs 10.98 ± 1.61 -fold at 10 μ M) which suggest that in this particular experimental setting **1u** acts as a full agonist.

Molecular modeling experiments were carried out to investigate the binding interactions between compounds (**1a**, **1d**, **1f**, **1j**, **1n**, **1u**, **5b**, and **7**) and FXR, which aimed to provide the molecular basis for further structural optimization (for details, see Supplementary data). The crystal structure of human FXR–fexaramine complex reveals that the ligand binding pocket is hydrophobic, long and narrow (for details, see Supplementary data). Figure 3A shows the interaction modes of four potent partial agonists (com-

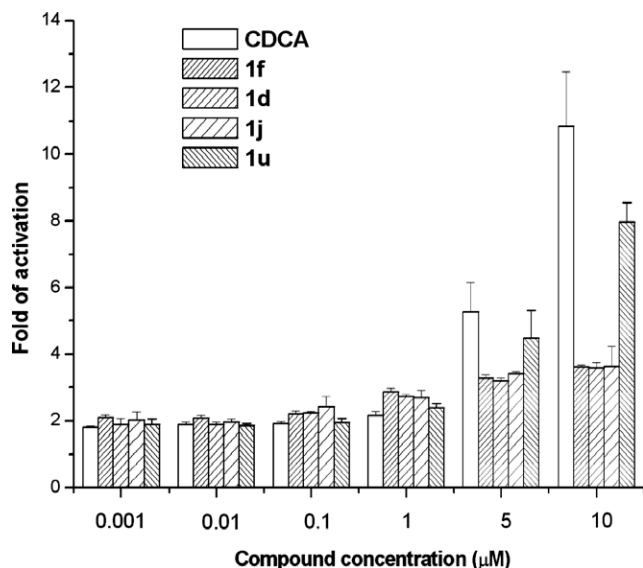


Figure 2. Concentration–response studies of four representative synthesized compounds **1f**, **1d**, **1j**, and **1u** using CDCA as a control.

pounds **1a**, **1d**, **1f**, and **1j**) with FXR ligand binding pocket. As seen in Figure 3A, these four compounds have similar binding modes. The pyrazolidine-3,5-dione core occupies the deep hydrophobic area, while the substituted N1 moiety points to the receptor's 'back door',¹² localized between loops H1–H2 and H5–H6. The pyrazolidine-3,5-dione core interacts with the protein residues through two hydrogen bonds with Leu291 from helix 3 and with Tyr365 from helix 7 respectively. In contrast, the O atom of the ether skeleton forms hydrogen bonding both with His298 from helix 3 and Ser336 from helix 5. At the same time, the two phenyl rings A and B of the agonists interact with the receptor via van der Waals interaction. The trifluoromethyl group of **1d**, on one hand, forms strong hydrophobic interaction with the residues from helix 2; on the other hand, it points to the space between helices 2 and 5 and has no steric hinder with residues from helix 5. This may contribute to its lower EC₅₀ value than **1a**. Compared with **1a**, the additional carbonyl group of the N1 substituents of **1f** and **1j** increases the length of these two compounds, which resulted in an extension

into the deeper hydrophobic binding pocket of FXR. This may in part explain the higher agonistic activities of **1f** and **1j** against FXR when compared to **1a**. Compared with the above compounds **1a**, **1d**, **1f**, and **1j**, **1n** has the *para*-substitution on the benzyl ring A. Because the binding pocket is hydrophobic, long and narrow, this different substitution results in a different binding mode (Fig. 3B) with the *meta*-substitution of the ring A (i.e., **1f** and **1j**). The *para*-substitution leads to an extended conformation of the ether oxygen group. This change leads to the loss of the hydrogen bonds formed between the ether oxygen atom and His298 and Ser336, which was observed in the *meta*-substituent compounds (**1f** and **1j**). This may in part account for the lower potency when compared to **1f** and **1j**.

In contrast to the above five compounds, the full agonist **1u** has a distinct structure. This implies **1u** may have different binding mode with the above compounds. This idea was supported by the binding conformations obtained by molecular docking. Compared to the above compounds, the two N atoms of pyrazolidine-3,5-dione core of **1u** is disubstituted by phenyl group. These two phenyl groups form an expanded conformation, and thereby can not extend into the deep binding pocket of FXR. One of carbonyl groups in pyrazolidine-3,5-dione core forms a hydrogen bond with His298, while the two phenyl rings form hydrophobic contacts with Met294, Phe340, Phe370, Met369, Leu352, and Ile356, as shown in Figure 3C.

Compounds **5b** and **7** also showed higher potency than CDCA. However, these two compounds have different structural sketch from the above four compounds (**1a**, **1d**, **1f**, and **1j**). Compared with pyrazolidine-3,5-dione derivative **1t** (EC₅₀ = 3.31 μM), compound **5b** was a precursor for the synthesis of **1t** with diethyl malonate moiety instead of pyrazolidine-3,5-dione core. These two ethyl ester groups form an extended conformation, which results in a bulky volume when compared with compounds **1t**. For this reason, this moiety of compound **5b** could not bind at the deep pocket formed by helix 12, 11, and 3, since the pocket inside the fold is too narrow and long to accommodate the groups of large size. From Figure 3D, compound **5b** forms two hydrogen bonds with His298 and Ser336 at one of its ethyl ester groups. The other ethyl ester group form hydrophobic interactions with Phe340, Phe370, Met369, Leu352, and Ile356. The benzyloxy moiety of compound **5b** extends into the deep binding pocket. This binding orientation is just contrary to that of aforementioned four compounds. In contrast with compound **1a–u**, compound **7** is shorter in length. Like

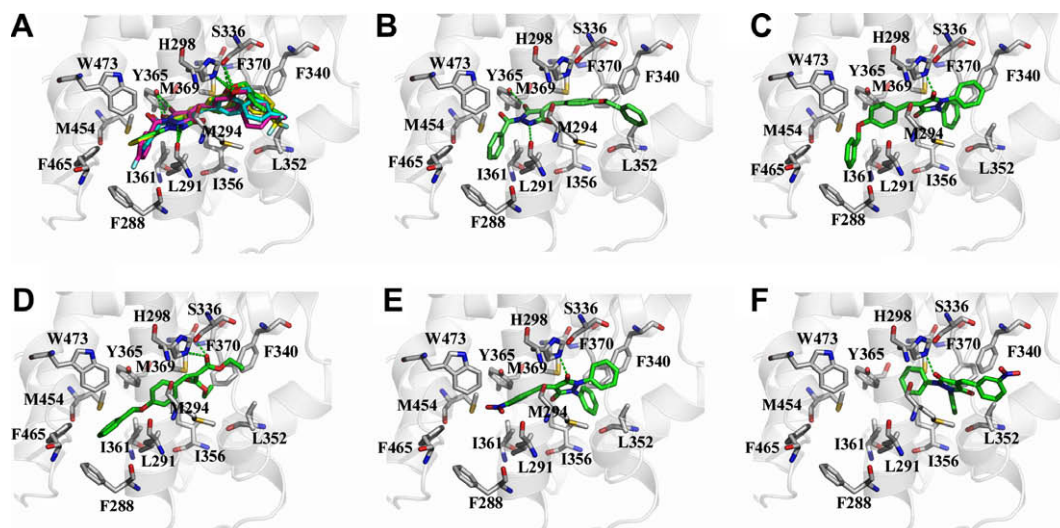


Figure 3. Close view of binding modes of high potent compounds in the binding pocket of human FXR (PDB code: 1OSH). Hydrogen bonds are represented by green dotted lines. Important residues are labeled. (A) compound **1a** (green); **1d** (yellow); **1f** (pink); and **1j** (cyan); (B) compound **1n**; (C) compound **1u**; (D) compound **5b**; (E) binding mode 1 of compound **7**; (F) binding mode 2 of compound **7**.

compound **1u**, these two phenyl groups also form an extended conformation. The docking results proposed two distinct binding modes existed for compound **7**, as shown in Figure 3E and F. In both binding modes, one of carbonyl groups in pyrazolidine-3,5-dione core forms a hydrogen bond with His298. However, the orientation of nitrobenzyl group differs a lot. In binding mode Figure 3E, the nitrobenzyl group binds in the deep pocket of FXR, whereas in binding mode Figure 3F, the same group points to the 'back door'. Regardless of the distinct binding modes, one of *N*-phenyl group on pyrazolidine-3,5-dione core points to the vacuum and forms hydrophobic contacts with Met294, Phe340, Phe370, Met369, Leu352, and Ile356. Although only one hydrogen bond forms between compound **7** and ligand binding pocket, the strong hydrophobic interactions formed by its phenyl ring compensates in part the loss in hydrogen bonding interaction. This may account for the high potency of compound **7**.

In summary, a novel hit compound (**1a**) was discovered by means of virtual screening techniques. Starting from the hit, a series of compounds have been rapidly generated by microwave techniques and evaluated by a cell-based luciferase transactivation assay with the aim of identifying potential FXR agonists endowed with positive pharmacological profile in the treatment of metabolic diseases. Among all the tested compounds, 12 compounds exhibited potent partial or full agonistic activities compared to that of the reference drug (CDCA), with EC₅₀ values between 1.86 and 6.92 μM. Molecular modeling studies for selected compounds were also presented to reveal the binding interactions between the ligands and receptors and the information is useful for the further lead optimization.

Acknowledgments

We gratefully acknowledge financial support from the State Key Program of Basic Research of China (Grant 2006BAI01B02), the National Natural Science Foundation of China (Grants 30672539 and 20721003), and the 863 Hi-Tech Program of China (Grant 2006AA020602).

Supplementary data

Supplementary data associated with this article can be found, in the online version, at doi:10.1016/j.bmcl.2008.09.027.

References and notes

- Cariou, B.; Staels, B. *J. Hepatol.* **2006**, *44*, 1213.
- Wang, H.; Chen, J.; Hollister, K.; Sowers, L. C.; Forman, B. M. *Mol. Cell* **1999**, *3*, 543.
- Makishima, M.; Okamoto, A. Y.; Repa, J. J.; Tu, H.; Learned, R. M.; Luk, A.; Hull, M. V.; Lustig, K. D.; Mangelsdorf, D. J.; Shan, B. *Science* **1999**, *284*, 1362.
- Parks, D. J.; Blanchard, S. G.; Bledsoe, R. K.; Chandra, G.; Consler, T. G.; Kliewer, S. A.; Stimmel, J. B.; Willson, T. M.; Zavacki, A. M.; Moore, D. D.; Lehmann, J. M. *Science* **1999**, *284*, 1365.
- Chen, W.; Owsley, E.; Yang, Y.; Stroup, D.; Chiang, J. Y. *J. Lipid. Res.* **2001**, *42*, 1402.
- Lew, J. L.; Zhao, A.; Yu, J.; Huang, L.; De Pedro, N.; Pelaez, F.; Wright, S. D.; Cui, J. *J. Biol. Chem.* **2004**, *279*, 8856.
- Willson, T. M.; Jones, S. A.; Moore, J. T.; Kliewer, S. A. *Med. Res. Rev.* **2001**, *21*, 513.
- Pellicciari, R.; Costantino, G.; Fiorucci, S. *J. Med. Chem.* **2005**, *48*, 5383.
- Westin, S.; Heyman, R. A.; Martin, R. *Mini-Rev. Med. Chem.* **2005**, *5*, 719.
- Lee, F. Y.; Lee, H.; Hubbert, M. L.; Edwards, P. A.; Zhang, Y. *Trends Biochem. Sci.* **2006**, *31*, 572.
- Pellicciari, R.; Fiorucci, S.; Camaioni, E.; Clerici, C.; Costantino, G.; Maloney, P. R.; Morelli, A.; Parks, D. J.; Willson, T. M. *J. Med. Chem.* **2002**, *45*, 3569.
- Pellicciari, R.; Gioiello, A.; Costantino, G.; Sadeghpour, B. M.; Rizzo, G.; Meyer, U.; Parks, D. J.; Entrena-Guadix, A.; Fiorucci, S. *J. Med. Chem.* **2006**, *49*, 4208.
- Maloney, P. R.; Parks, D. J.; Haffner, C. D.; Fivush, A. M.; Chandra, G.; Plunket, K. D.; Creech, K. L.; Moore, L. B.; Wilson, J. G.; Lewis, M. C.; Jones, S. A.; Willson, T. M. *J. Med. Chem.* **2000**, *43*, 2971.
- Downes, M.; Verdecia, M. A.; Roecker, A. J.; Hughes, R.; Hogenesch, J. B.; Kast-Woelbern, H. R.; Bowman, M. E.; Ferrer, J. L.; Anisfeld, A. M.; Edwards, P. A.; Rosenfeld, J. M.; Alvarez, J. G.; Noel, J. P.; Nicolaou, K. C.; Evans, R. M. *Mol. Cell* **2003**, *11*, 1079.
- Zhang, T.; Zhou, J.-H.; Shi, L.-W.; Zhu, R.-X.; Chen, M.-B. *Bioorg. Med. Chem. Lett.* **2007**, *17*, 2156.
- Deng, G.; Liu, Z.; Ye, F.; Luo, X.; Zhu, W.; Shen, X.; Liu, H.; Jiang, H. *Eur. J. Med. Chem.*, in press, doi:10.1016/j.ejmech.2008.01.032.
- Zhang, J.; Xu, Y. C.; Shen, J. H.; Luo, X. M.; Chen, J. G.; Chen, K. X.; Zhu, W. L.; Jiang, H. L. *J. Am. Chem. Soc.* **2005**, *127*, 11709.
- Zhang, J.; Yu, K.; Zhu, W.; Jiang, H. *Bioorg. Med. Chem. Lett.* **2006**, *16*, 3009.
- Ewing, T. J.; Makino, S.; Skillman, A. G.; Kuntz, I. D. *J. Comput. Aided Mol. Des.* **2001**, *15*, 411.
- Li, J.; Chen, J.; Gui, C. S.; Zhang, L.; Qin, Y.; Xu, Q.; Zhang, J.; Liu, H.; Shen, X.; Jiang, H. L. *Bioorg. Med. Chem.* **2006**, *14*, 2209.
- Rarey, M.; Kramer, B.; Lengauer, T.; Klebe, G. *J. Mol. Biol.* **1996**, *261*, 470.
- Lipinski, C. A.; Lombardo, F.; Dominy, B. W.; Feeney, P. J. *Adv. Drug Deliv. Rev.* **1997**, *23*, 3.
- Zheng, S. X.; Luo, X. M.; Chen, G.; Shen, J. H.; Jiang, H. L.; Chen, K. X. *J. Chem. Inform. Model.* **2005**, *45*, 856.
- Li, Z.; Liao, C.; Ko, B. C. B.; Shan, S.; Tong, E. H. Y.; Yin, Z.; Pan, D.; Wong, V. K. W.; Shi, L.; Ning, Z.-Q.; Hu, W.; Zhou, J.; Chung, S. S. M.; Lu, X.-P. *Bioorg. Med. Chem. Lett.* **2004**, *14*, 3507.